6061

An NMR, X-ray crystal structure, and molecular mechanics study of di-(3-deoxy-D-*glycero*-pentulose) 1,2′ : 2,1′ dianhydride

Abstract

The structure of di-(3-deoxy-D-*glycero*-pentulose), 1,2′ : 2,1′ dianhydride, $C_{10}H_{16}O_6$, has been studied by NMR spectroscopy in D_2O and Me_2SO-d_6 solutions, by X-ray crystal-structure analysis at 123 K, and by molecular mechanics calculations. The NMR data show that the molecule is asymmetric with distinct resonances that can be assigned to all hydrogens and protonated carbon atoms. In the crystal, the central dioxane ring has a chair conformation. Both furanoid rings have envelope conformations, one is ^3E, the other E_O. The molecular mechanics calculations indicate a marked difference in the pseudorotational flexibility in the two furanoid rings. The ^3E (α-anomeric) ring is relatively restricted, with $^3T_2$–^3E–$^3T_4$ conformations within 1 kcal/mol from the energy minimum. The E_O (β-anomeric) ring is much more flexible, with conformations from $^5T_4$ through E_O to $^4T_3$, within the 1 kcal/mol energy contour. This result is consistent with the NMR data. For the ^3E ring, the NMR dihedral angles, calculated from coupling constants, are consistent with conformations from ^3E to $^5T_4$, while for the E_O ring they range from $^3T_4$–^2T_O. By decomposing the calculated energy components, the difference in the pseudorotational flexibility of the two furanoid rings can be related to the difference in the torsion angle energies about the C-5–O-5 bonds in the two rings. The molecules in the crystal are linked by infinite chains of hydrogen bonds.

1. Introduction

A new disaccharide, **1**, has been prepared and tentatively characterized as di-(3-deoxy-D-*glycero*-pentulose) 1,2′ : 2,1′ dianhydride, from the elemental analysis and its IR spectrum. This compound is analogous to the known di-D-fructose dianhydride reported by Lemieux and Nagarajan [1]. The monomer, 2-deoxy-D-*glycero*-pentulose, is a minor component (1–2.5%) of the carbohydrate mixture resulting from the alkaline treatment of aqueous lactulose solutions. Its structure has been suggested by Anderson [2] as the product of the reaction of "3-deoxy-xylitol" with L-iditol dehydrogenase. The present study was undertaken to establish the molecular structure of **1** and to compare its solution and solid-state conformations.

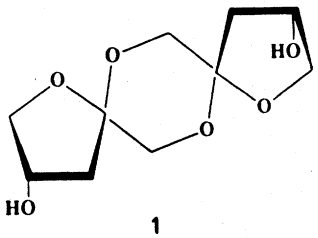

1

2. Experimental

*Isolation and purification of di-(3-deoxy-*D*-*glycero*-pentulose) 1,2′ : 2,1′ dianhydride.* (**1**)—3-Deoxy-D-*glycero*-pentulose is a minor component (1–2.5%) of the carbohydrate mixture resulting from alkaline treatment of aqueous lactose solutions. It was isolated from such solutions * by solvent extraction with either acetone or butanone and subsequent column chromatography on a Ca^{2+} form of a sulfated polystyrene cation-exchange resin, using water as eluent. It eluted after all other sugars except for tagatose, which co-eluted. It was obtained as an oily mixture of anomers, which could not be induced to crystallize. After prolonged storage, the water-free oil crystallized as the dimer (**1**); mp 148–149° C; $[\alpha]_D^{20}$ + 12.0° (*c* 2.3, H_2O). Anal. Calcd for $C_{10}H_{16}O_6$: C, 51.72; H, 6.94; O, 41.34. Found: C, 51.35; H, 6.83; O, 41.2%.

Solution state NMR spectra and assignments.—The ^1H and ^{13}C NMR spectra were obtained on Jeol GX-400 and Bruker MSL 300 NMR spectrometers. A 15-mg sample of **1**, dissolved in Me_2SO-d_6 or D_2O, was used for the NMR experiments. All chemical shifts are reported relative to Me_4Si using the CH_3 resonance of Me_2SO-d_6 as the secondary standard (39.5 ppm for ^{13}C, 2.49 ppm for ^1H). The proton NMR spectrum was obtained at 400 MHz. The spectrum was obtained from eight scans (90° pulse width) with a 2-s recycle time. The spectral width was 1800 Hz with 16 K data points.

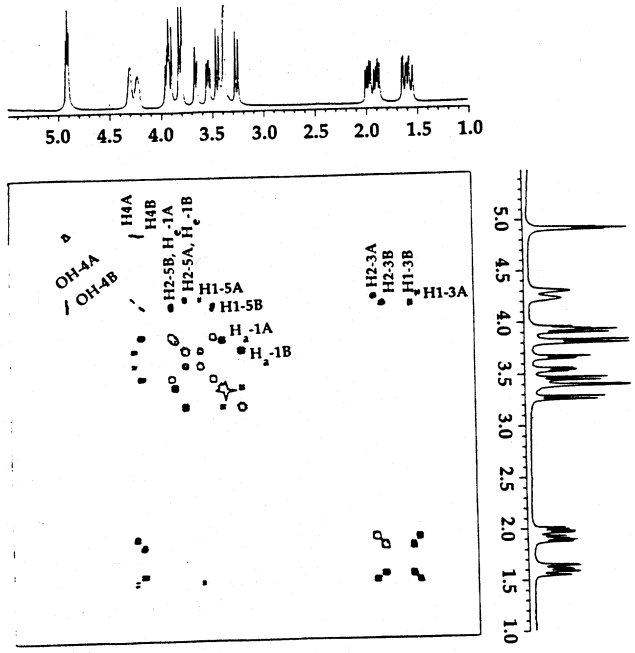

Fig. 1. 2D homonuclear COSY spectrum of **1** in Me_2SO-d_6.

The proton homonuclear 2D-COSY and 2D-NOESY spectra were obtained on a Jeol GX-400 instrument operating at 400 MHz. The sweep width in both dimensions was 1800 Hz with 2 K points in the F_1 dimension and 512 points in the F_2 dimension. The data were transformed using a sine-bell function in both dimensions.

The 2D-HETEROCOSY spectrum was also obtained on the Bruker MSL-300 operating at 75 MHz for ^{13}C. The sweep width in the F2 dimension was 5102 Hz with 1 K data points and in the F_1 dimension 515 Hz with 256 data points. The F_1 dimension was zero-filled to 512 points. The data were transformed using a sine-bell function in both dimensions.

2D-NOESY experiments were carried out in Me_2SO-d_6 at 400 MHz. The spectra were obtained with a spectral width of 1800 Hz, a 2 K × 512 matrix and a mixing time of 200 ms. Each spectrum required 32 scans. All data were processed using a sine-bell apodization function.

The 2D homonuclear COSY spectrum in Me_2SO-d_6, shown in Fig. 1, has a unique shift for each protonated carbon and hydrogen atom, confirming that the conformation of the molecule is asymmetric in solution. Two separate OH resonances (4.92 δ, 4.90 δ) are observed due to slow exchange of OH in Me_2SO. The higher field ^1H resonance (less hydrogen-bonded) was assigned to O-4B, since the crystal structural analysis showed that this OH had the greater thermal motion in the crystal. This preliminary assignment was later justified by the consistency of subsequent assignments. The assignment of the proton resonances for the hydrogens attached to C-3, C-4, and C-5 for each ring were made from the connectivities

Table 1
NMR chemical shift assignments and coupling constants

Chemical shifts		Assignment	$J_{1,2}$(Hz)		$J_{1,3}$(Hz) to H-C4A	
D_2O	Me_2SO-d_6		D_2O	Me_2SO-d_6	D_2O	Me_2SO-d_6
1.80	1.59	H-1–C-3A	14.9	14.1	0.00	2.00
2.20	1.95	H-2–C-3A			6.59	6.80
4.02	3.67	H-1–C-5A	10.1	11.0	0.00	0.50
3.90	3.82	H-2–C-5A			3.95	6.00 to H-C4B
1.92	1.63	H-1–C-3B	14.5	14.6	0.00	3.90
2.05	1.89	H-2–C-3B			6.59	8.30
4.16	3.54	H-1–C-5B	10.0	9.2	2.64	5.90
3.92	3.94	H-2–C-5B			5.27	6.30
3.65	3.45	H_a–C-1A		11.7		
3.48	3.25	H_a–C-1B				
4.17	3.89	H_e–C-1A		11.7		
4.07	3.82	H_e–C-1B				
4.55	4.32	H–C-4A				
4.52	4.24	H–C-4B				
	4.92	H–O-4A				
	4.90	H–O-4B				

shown in Fig. 1. The proton resonances associated with the hydrogens on C-1A and C-1B were assigned by giving the axially oriented protons the higher chemical shift.

The chemical-shift assignments and coupling constants in Me_2SO-d_6 and D_2O solution are given in Table 1. Fig. 2 is the 2D ^1H, ^{13}C heteronuclear COSY spectrum in Me_2SO-d_6. All carbon atoms, with the exception of the nonprotonated C-2A and C-2B, were assigned resonances in accordance with those of the proton spectrum.

Fig. 3 is the ^1H NOESY spectrum in Me_2SO-d_6. The spectrum has cross-peaks between the OH resonances (at 4.92 δ and 4.90 δ) and the HDO resonance at 3.48 due to chemical exchange. The cross-peaks for the axial proton resonances on H_a-1A and H_a-1B are observed, but not for the equatorial protons. Cross-peaks for H_a-1A and H_a-1B are also observed in the COSY spectrum for the Me_2SO-d_6 solution, indicating long-range scalar coupling (0.77 Hz measured by 1D decoupling experiments) in addition to the through-space dipolar interaction. The H_a-1A to H_a-1B distance from the crystal-structure analysis is 3.77 Å. The other H ··· H distances across the dioxane ring from axial to equatorial and equatorial to equatorial are 3.92, 3.99, and 4.61 Å, respectively. The proton dihedral angles, discussed later in comparison with the crystal structure and molecular mechanics results, were obtained using the Karplus equation [3].

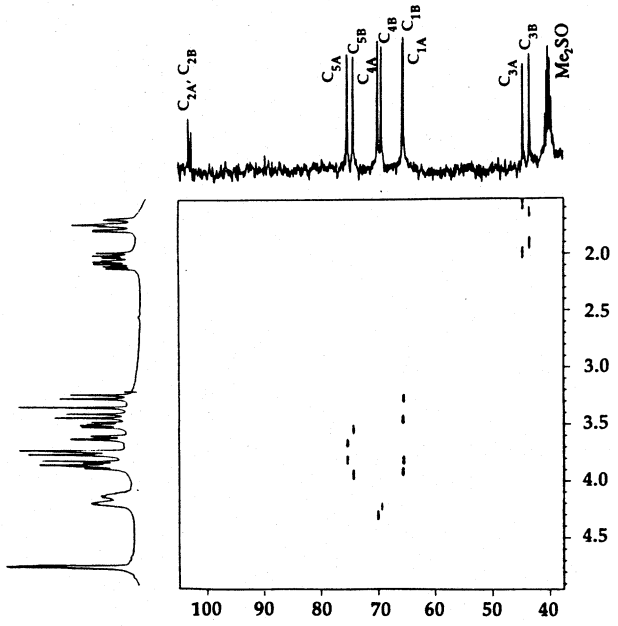

Fig. 2. 2D ^{1}H, ^{13}C heteronuclear COSY spectrum of **1** in Me_2SO-d_6.

Crystal-structure analysis.—Clear, plate-like crystals were obtained by recrystallization from methanol at 3° C. The crystallographic, structure determination, and refinement data are given in Table 2. The diffraction intensities were measured with a Nonius CAD-4 diffractometer at 123 K, using Ni-filtered Cu $K\alpha$ radiation by integrating $\omega/2\theta$ scans over 96 intervals. The structure was solved by direct methods, using the program SHELX [6], with E's greater than 1.2. The first E-map revealed the positions of all 16 nonhydrogen atoms. The 16 hydrogen atoms were located on difference Fourier maps. The analysis confirmed the configuration, **1**. The atomic notation and thermal ellipsoids are shown in Fig. 4, and the atomic parameters are given in Table 3 *.

Molecular mechanics calculations.—The MM3(92) molecular mechanics program was used throughout [7]. The block-diagonal optimizer option was used, as was a dielectric constant of 80.0, unless stated otherwise. An optimization that was started with the crystallographic coordinates in the order given in Table 3 reproduced the observed geometry closely, as shown in Table 4. The B ring in the molecular mechanics structure described in Table 4 has pseudorotated slightly in the direction of $^{2}T_{O}$, and the whole model has an energy 0.25 kcal/mol higher than the structure at the minimum found in the conformational search described below. The mean deviation of bond lengths in the dioxolane ring is 0.002 Å, less

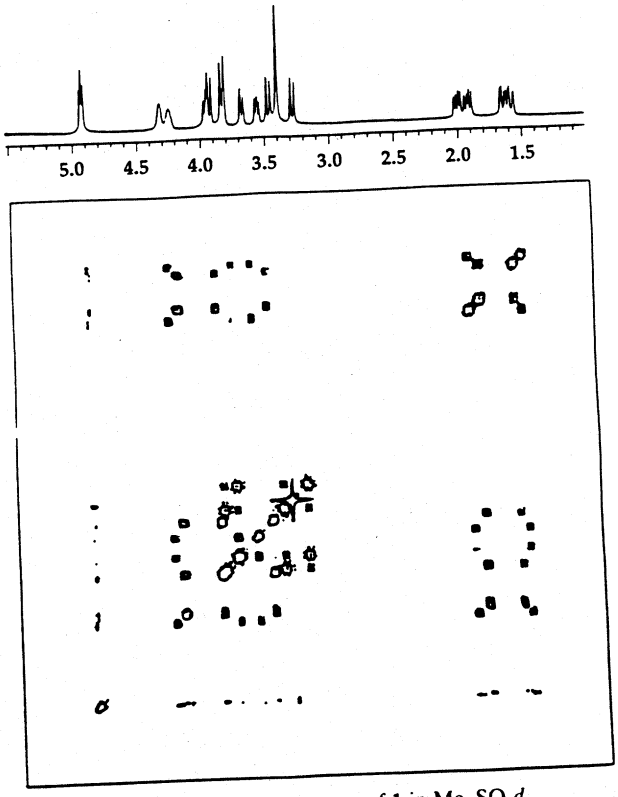

Fig. 3. ^{1}H NOESY spectrum of **1** in Me_2SO-d_6.

than the experimental standard deviation. The differences > 0.012 Å are for the four bonds to the oxygens of the furanoid rings and the two C-4–O-4 bonds which are all predicted to be too long by 0.016 to 0.019 Å. The calculated conformation for the dioxane ring was very close to that observed in the crystal, with mean absolute deviation in ring torsion angles of 1.5°. Deviations were 4.4 and 6.0° for the A and B rings, respectively.

Optimizations started under different conditions gave almost constant results for the dioxolane ring and A ring but the resulting parameters for the B ring were more varied. In particular, optimizing with the coordinates in a different order and the full-matrix option of MM3 bypassed the local minimum near the crystal structure corresponding to the structure in Table 4 and gave a B ring close to the global minimum in energy. Restraining the C-4A–C-5A–O-5A–C-2A and C-2B–C-3B–C-4B–C-5B torsion angles to their crystallographic values during optimization did not diminish the other discrepancies among the observed and predicted values in Table 4, nor was a dielectric constant of 4 helpful in resolving the discrepancies.

The extreme sensitivity of the resulting structure to the exact details of the optimization is caused by a very flat potential energy surface for the B ring. In

Table 2
Crystal data and X-ray diffraction analysis data for di-(3-deoxy-D-*glycero*-pentulose) 1,2′:2,1′ dianhydride

Crystal data
$C_{10}H_{16}O_6$, mol wt 232.238, $P2_12_12_1$, $Z = 4$
Cell dimensions at 123 K [293 K]: $a = 5.588(1)$ [5.653(1)], $b = 12.806(1)$ [12.855(1)], $c = 15.196(2)$ [15.258(2)] Å
$V = 1087.29$ [1108.72] Å^3, based on 25 reflections with $24° < \theta < 30°$, using Ni-filtered Cu $K\alpha$ radiation, $\lambda = 1.5418$ Å, $\mu = 8.85$ [9.02] cm^{-1}
$D_x = 1.412$ [1.392] g cm^{-3}, $D_m = [1.385]$ g cm^{-3}
Structure determination and refinement data
Crystal dimensions, $0.48 \times 0.25 \times 0.18$ mm
No. of reflections measured, 1534
No. of unique reflections, 1301
No. of observed reflections, 1250, $F_{obs} > 2\sigma(F_{obs})$
Range of h, k, l: $0 \le h \le 6$, $0 \le k \le 14$, $0 \le l \le 17$
$\theta_{max} = 60°$, observation : parameter ratio = 5.98
Residual electron difference density, ± 0.15 eÅ^{-3}
Final agreement factors:
$R(F) = 0.032$, $wR(F) = 0.048$, S (goodness of fit) = 1.79
Function minimized: $R = \Sigma[w(k\|F_0\| - \|F_c\|)^2]$, using UPALS [a], $w = 1/[\sigma^2(F) + (0.02F_0)^2]$; $\sigma(F)$ based on counting statistics
Intensity data were processed using the program BUFFALO [b]

[a] Ref 4. [b] Ref 5.

molecular mechanics, atoms are moved sequentially during optimization and thus different atomic orders in the input lead to different results. In this case, the energy consequences are minimal. However, differences in atomic order can cause larger differences when the starting structure is at a saddle point of the multidimensional energy hypersurface.

To explore the conformational flexibility of the furanoid rings, the two furanoid rings were modelled separately with the adjacent dioxolane ring attached in the chair conformation observed in the crystal structure. Starting models were pre-

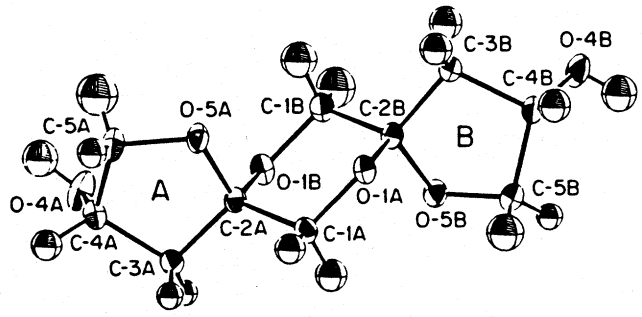

Fig. 4. Conformation and atomic notation of 1 from crystal-structure analysis at 123 K. The thermal ellipsoids are at 50% probability.

Table 3
Atomic positional parameters and equivalent thermal parameters for the crystal structure of di-(3-deoxy-D-*glycero*-pentulose) 1,2′:2,1′ dianhydride at 123 K [a]

Atom	x/a	y/b	z/c	B_{eq}(Å^2) [b]
O-1A	$506(3)\times10^{-4}$	$7375(1)\times10^{-4}$	$-3875(1)\times10^{-4}$	$139(3)\times10^{-2}$
C-1A	−1385(4)	6893(1)	−4367(1)	147(4)
C-2A	−739(4)	5790(1)	−4639(1)	134(4)
C-3A	−2715(4)	5232(2)	−5139(1)	159(4)
C-4A	−1364(4)	4492(2)	−5751(1)	163(4)
C-5A	962(4)	5077(2)	−5909(1)	196(4)
O-4A	−1030(3)	3528(1)	−5307(1)	225(4)
O-5A	1247(3)	5823(1)	−5216(1)	177(3)
O-1B	−166(3)	5198(1)	−3871(1)	158(3)
C-1B	1716(4)	5670(1)	−3373(1)	168(4)
C-2B	1169(3)	6794(1)	−3115(1)	132(4)
C-3B	3245(4)	7378(2)	−2697(1)	159(4)
C-4B	2076(4)	8058(2)	−1984(1)	158(4)
C-5B	−585(4)	7818(2)	−2084(1)	184(4)
O-4B	2976(3)	7745(2)	−1152(1)	281(4)
O-5B	−691(3)	6804(1)	−2483(1)	168(3)
H-O-4A	$-11(5)\times10^{-3}$	$312(2)\times10^{-3}$	$-562(2)\times10^{-3}$	
H-1-C-1A	−171(5)	731(2)	−486(2)	
H-2-C-1A	−284(5)	689(2)	−399(2)	
H-1-C-3A	−381(4)	493(2)	−474(2)	
H-2-C-3A	−348(5)	576(2)	−551(2)	
H-C-4A	−221(5)	435(2)	−632(2)	
H-1-C-5A	230(7)	460(3)	−583(2)	
H-2-C-5A	97(5)	548(2)	−647(2)	
H-O-4B	231(6)	807(2)	−77(2)	
H-1-C-1B	322(6)	564(2)	−369(2)	
H-2-C-1B	205(6)	517(2)	−285(2)	
H-1-C-3B	443(5)	684(2)	−242(2)	
H-2-C-3B	409(5)	777(2)	−317(2)	
H-C-4B	247(5)	877(2)	−215(2)	
H-1-C-5B	−140(5)	834(2)	−251(2)	
H-2-C-5B	−131(5)	777(2)	−151(2)	

[a] Esd values given in parentheses refer to the least significant digit. [b] $B_{eq} = 4.3(\Sigma_{ij} B_{ij} a_i a_j)$, calculated from the refined, anisotropic thermal parameters.

pared by optimizing the furanoid–pyranoid systems with all of the furanoid ring atoms constrained in a plane (with $z = 0$). Atoms C-3 and C-5 were than raised and lowered from the ring plane to ±0.9 Å in increments of 0.1 Å, to generate 361 different ring conformations. The heights of the substituent hydrogen atoms followed the ring atoms. Each of these distorted conformations was then optimized, keeping the z-coordinates of the atoms of the furanoid ring fixed, but allowing full optimization of all other coordinates of all atoms. A dielectric constant of 80 was used, to eliminate any effects of hydrogen bonding and best emulate an aqueous environment. Optimizations ended when the energy for these 23-atom molecules changed less than 1.84 cal per five iterations, which is the

Table 4
Bond lengths and selected valence and torsion angles in di-(3-deoxy-D-*glycero*-pentulose) 1,2′:2,1′ dianhydride
Crystal structure (at 123 K) vs. molecular mechanics [a]

	Crystal Structure	MM		Crystal Structure	MM
Bond lengths (Å)					
dioxane ring					
C-1A–C-2A	1.516	1.519	C-1B–C-2B	1.522	1.520
C-1A–O-1A	1.434	1.433	C-1B–O-1B	1.430	1.433
C-2A–O-1B	1.426	1.425	C-2B–O-1A	1.424	1.426
furanoid rings					
C-2A–C-3A	1.519	1.525	C-2B–C-3B	1.520	1.537
C-3A–C-4A	1.527	1.517	C-3B–C-4B	1.535	1.533
C-4A–C-5A	1.519	1.531	C-4B–C-5B	1.526	1.528
C-2A–O-5A	1.414	1.432	C-2B–O-5B	1.415	1.434
C-5A–O-5A	1.431	1.449	C-5B–O-5B	1.435	1.444
exocyclic					
C-4A–O-4A	1.419	1.435	C-4B–O-4B	1.418	1.426
Selected valence angles (°)					
O-5A–C-2A–O-1B	110.3	110.9	O-5B–C-2B–O-1A	110.8	111.7
C-2A–O-5A–C-5A	110.4	108.7	C-2B–O-5B–C-5B	105.4	105.0
C-1A–O-1A–C-2B	112.9	111.9	C-1B–O-1B–C-2A	111.9	111.8
C-2A–C-3A–C-4A	103.7	102.6	C-2B–C-3B–C-4B	104.4	105.0
C-3A–C-4A–C-5A	102.3	101.3	C-3B–C-4B–C-5B	103.3	103.1
Selected torsion angles (°)					
dioxane ring					
C-1A–O-1A–C-2B–C-1B	52.7	56.4	O-1A–C-2B–C-1B–O-1B	−52.3	−55.7
C-2A–C-1A–O-1A–C-2B	−56.6	−56.6	C-1B–O-1B–C-2A–C-1A	−56.5	−56.8
O-1B–C-2A–C-1A–O-1A	56.7	56.5	C-2B–C-1B–O-1B–C-2A	55.8	57.1
furanoid rings					
O-5A–C-2A–C-3A–C-4A	29.7	36.4	O-5B–C-2B–C-3B–C-4B	−22.0	−29.7
C-2A–C-3A–C-4A–C-5A	−29.6	−36.1	C-2B–C-3B–C-4B–C-5B	−1.6	7.5
C-3A–C-4A–C-5A–O-5A	20.1	24.6	C-3B–C-4B–C-5B–O-5B	24.4	17.0
C-4A–C-5A–O-5A–C-2A	−1.8	2.4	C-4B–C-5B–O-5B–C-2B	−39.6	−36.8
C-5A–O-5A–C-2A–C-3A	−17.6	21.5	C-5B–O-5B–C-2B–C-3B	38.5	41.4
interring					
C-5A–O-5A–C-2A–O-1B	99.9	95.3	C-5B–O-5B–C-2B–O-1A	−76.3	−75.5
O-1A–C-1A–C-2A–C-3A	−178.0	176.1	O-1B–C-1B–C-2B–C-3B	172.0	−175.7
ring-exocyclic					
C-2A–C-3A–C-4A–O-4A	90.1	79.5	C-2B–C-3B–C-4B–O-4B	117.6	123.9

[a] Esd values are 0.003 Å for bond lengths, 0.2° for valence and torsion angles.

default termination criterion. The optimized coordinates of the furanoid atoms were used to calculate the Cremer–Pople puckering parameters. After conversion of the puckering parameters from polar to Cartesian coordinates, the corresponding energies were plotted and contoured with SURFER to give the results shown in Fig. 5.

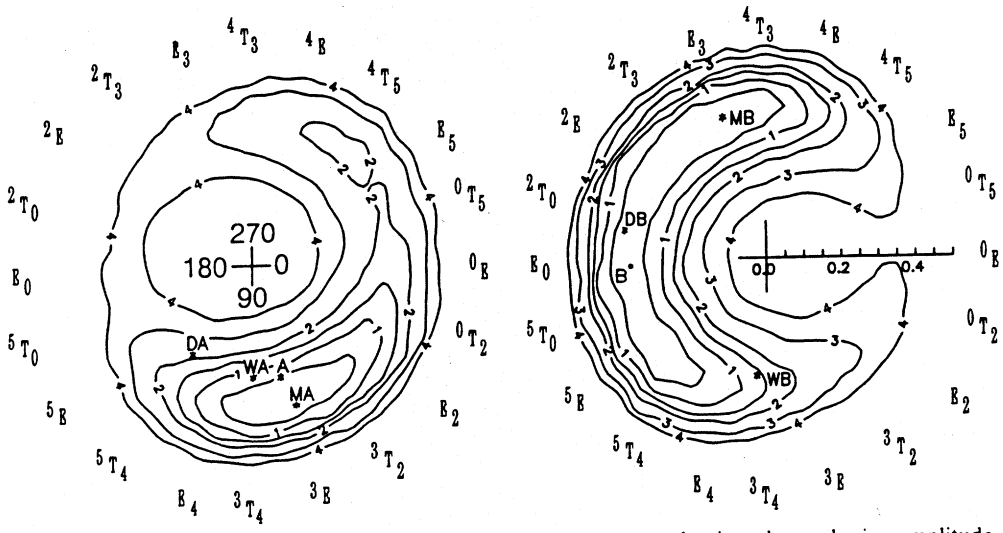

Fig. 5. Energy surface for the A and B furanoid rings. The linear scale gives the puckering amplitude. The contours are at 0.5 to 2.0, then 3.0, 4.0 kcal/mol. The ring conformations are given on the circumference. The calculated energy minima are at MA and MB. The crystal, D_2O, and Me_2SO conformations are at A, WA, DA, B, WB, and DB, respectively.

The best-fit models to the experimental NMR dihedral angles were constructed by applying the signs from the crystal structure and constraining the C-1–C-2–C-3–C-4 and C-3–C-4–C-5–O-5 torsion angles for each furanoid ring to values which gave the minimal discrepancy with the NMR and H–C–C–H dihedral angles. The values of these angles were monitored using CHEM-X while interactively changing the ring torsion angles, with the rings broken at O-5–C-2. The rings were then

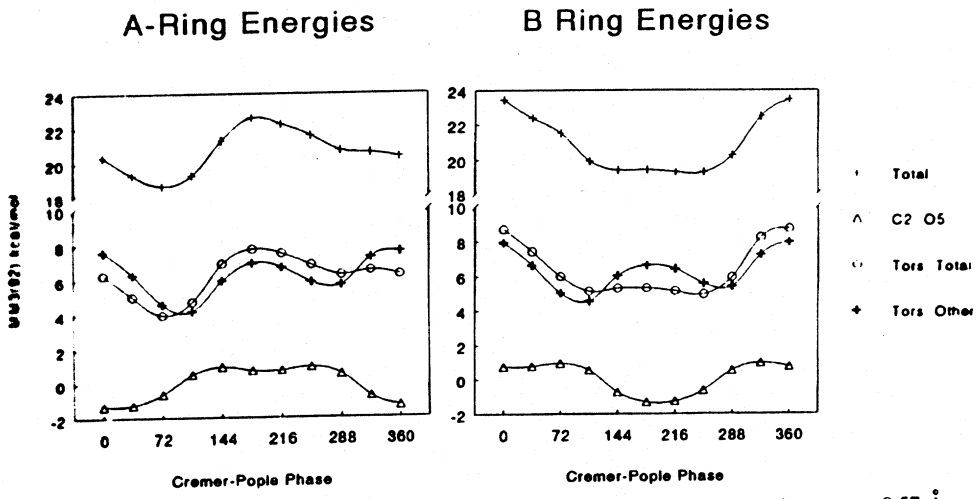

Fig. 6. Decomposition of energy components for the furanoid rings; envelope displacements 0.57 Å out of plane (q = 0.38 Å).

reformed and the structures were optimized using MM3, while retaining the ring torsion angles at the best-fit values.

In an effort to understand the basis for the difference in the pseudorotational flexibility of the two furanoid rings, we examined the energy components of the set of envelope conformations with puckering amplitudes of 0.38 Å. The 10 envelope forms were generated with four of the ring atoms held in the $z = 0$ plane and the out-of-plane atom held 0.57 Å above or below the plane with the dioxolane ring attached. The calculated energies were disected into four components; the total, the torsional, 1,4 van der Waals, and other van der Waals, as shown in Fig. 6.

3. Discussion

Molecular structure in the crystal.—As shown in Fig. 4, the molecule consists of two furanoid rings linked through the carbon atoms C-2A, C-2B of the central dioxane ring. The conformation of the dioxane ring is close to a perfect $^{1B}C_{1A}$ chair with Cremer–Pople puckering parameters Q = 0.538(2) Å, $\theta = 176.2°$. This is the conformation favored by the exo-anomeric effect with O-5–C-2–O-1–C-1 torsion angles of $\approx 60°$ (observed -68, $+63°$). With the alternative $^{1A}C_{1B}$ chair conformation these angles would be $\approx 180°$. A MM3(92) energy calculation for this alternative conformation gave a substantially higher energy (by 7.5 kcal/mol). Both furanoid rings have envelope conformations. The A (α-fructose) ring is $_3E$ with C-3A *exo* to C-4A–O-4A at 0.48 Å from C-2A–O-5A–C-5A–C-4A, which is planar within 0.01 Å (torsion angle $-1.8°$). The B (β-fructose) ring is E_O with O-5B *endo* to C-4B–O-4B at 0.54 Å from C-2B–C-3B–C-4B–C-5B, which is also planar within 0.01 Å (torsion angle $-1.6°$). The O-1A–C-1A–C-2A–C-3A and O-1B–C-1B′–C-2B–C-3B torsion angles are $-178°$ and 172°, respectively. This places the methylene C–H bonds on the C-1 atoms in a staggered orientation with respect to the C-2–C-3 bonds of the furanose rings.

The bond lengths, given in Table 4, are normal, with C–C between 1.516 and 1.535 Å (mean 1.523 Å) and C–O between 1.414 and 1.435 Å. In both C–O–C–O–C acetal sequences, the two inner bonds are shorter than the outer bonds by 0.011 and 0.015 Å, respectively. The corresponding C-5–O-5–C-2–O-1 torsion angles are $+100°$ in ring A and $-76°$ in ring B. The O-4 and O-5 distances are 3.205 and 3.121 Å for rings A and B, respectively. The syndiaxial interactions across the furanoid rings are different. For ring A, O-4A is 3.093 Å from O-1B, whereas for ring B, O-4′B is 4.353 Å from C-1B.

Thermal motion in the crystal.—A prominent feature of the molecular mechanics calculations, shown in Fig. 5, is a difference in the flexibility of the two furanoid rings. With the exception of the O-4 atoms, the mean B_{eq} values for the atoms in the two furanoid rings are almost equal, 159 vs. 161. There is, however, a 25% difference in those for the O-4 atoms. This difference is in the thermal motion normal to the mean plane of the rings. For O-4B, the root mean square displacement is 0.20 Å, vs. 0.09 Å for O-4A, corresponding to a more flexible B ring, as predicted.

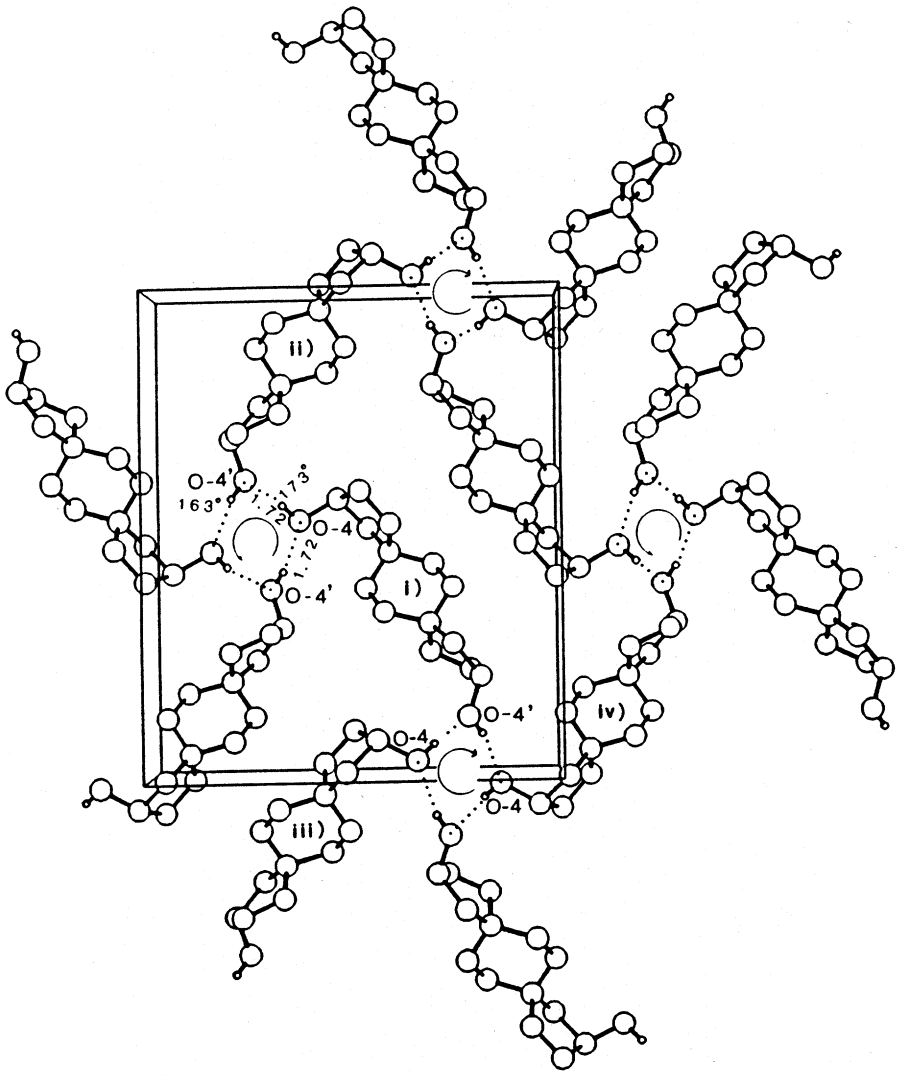

Fig. 7. Molecular packing in the crystal structure of **1**, viewed down the *a* axis with *b* horizontal. Symmetry code: (i) x, y, z; (ii) $1/2-x, 1-y, 1/2+z$; (iii) $1/2-x, -y, -1/2+z$; (iv) $-x, 1/2+y, 1/2-z$.

Molecular packing and hydrogen bonding in the crystal.—The molecular packing is shown in Fig. 7. The hydroxyl groups at each end of the molecule are linked by cooperative infinite chains of O-H · · · O bonds which form a spiral extending in the direction of the *a* axis. When the O–H covalent bond lengths are normalized to 0.97 Å, to correct for the electronic charge distribution, both O-4A–H · · · O-4B and O-4B–H · · · O-4A hydrogen bond lengths are 1.72(3) Å. The O-4A–H · · · O-4B and O-4B–H · · · O-4A are 173(3) and 163(3)°, respectively.

This arrangement corresponds to a strong cooperative system of intermolecular bonds which could cause some strain in the conformation of furanoid rings through the orientation of the C-OH bonds.

4. Comparison of the results

The comparison of the crystal structure and NMR data with the results of the MM3 furanoid ring optimizations is shown in Fig. 5 and Table 5. The agreement between the crystal structure conformations for the furanoid rings and the molecular mechanics calculations is excellent, with the observed conformations for rings A and B lying at 0.5 kcal/mol or less from the calculated energy minima, MA and MB. The correspondence regarding the flexibility of the two rings predicted by the molecular mechanics and the spread of solution conformations is also satisfactory. Only the NMR conformations in Me_2SO,DA, and in D_2O, WB, lie above the 1 kcal/mol contour.

The agreement between the H–C–C–H angles from the NMR results, the crystal structure analysis, the optimized molecular mechanics, and model-constrained molecular mechanics computations are shown in Table 5. The mean

Table 5
Comparison of NMR, crystal structure, and molecular mechanics data for vicinal proton interactions

H–C–C–H	NMR Dihedral angles (°)		Torsion angles (°)			
			Crystal	Molecular mechanics [a]		
	D_2O	Me_2SO				
				MA	WA	DA
Ring A						
H-1-C-3-H-C-4	90	117	+89	+81	+84	+91
H-2-C-3-H-C-4	26	23	−37	−40	−35	−27
H-1-C-5-H-C-4	90	107	−106	−92	−89	−86
H-2-C-5-H-C-4	45	30	+24	+28	+31	+34
C-2-C-3-C-4-C-5			−30	−6	−31	−23
C-2-O-5-C-5-C-4			−2	−4	−14	−25
				MB	WB	DB
Ring B						
H-1-C-3-H-C-4	90	131	+123	+112	+85	+129
H-2-C-3-H-C-4	26	0	+1	−7	−34	+9
H-1-C-5-H-C-4	123	142	−107	−90	−92	−102
H-2-C-5-H-C-4	36	28	+20	+32	+28	+19
C-2-C-3-C-4-C-5			−40	−36	−30	+8
C-2-O-5-C-5-C-4			−2	−4	−10	−38
Ring A Conformation			^3E	$^3T_2$–$^3T_4$ [b]	$^3T_4$	$^5T_4$
Ring B Conformation			E_O	$^5T_4$–$^4T_3$ [b]	$^3T_4$	$^2T_0$

[a] MA, MB: molecular mechanics minimization; WA, WB: best models for D_2O solution NMR data; DA, DB: best models for Me_2SO-d_6 solution NMR data. [b] Range of ring conformations less than 1 kcal/mol above minimum.

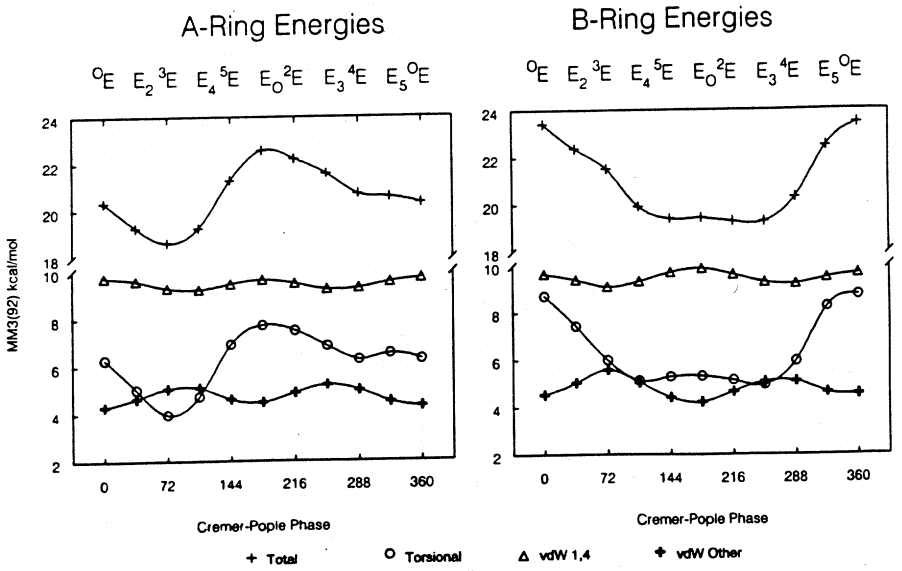

Fig. 8. Decomposition of the torsional energy components.

angular discrepancies between the model dihedral angles and the crystal values are 9° for both rings. For the NMR data the mean discrepancy is the same for the A ring, but larger, 14°, for the B ring. Since the NMR values correspond to a time average of the range of ring conformations, this is consistent with the greater flexibility of the B ring.

The results shown in Fig. 6 indicate that the principal difference between the A and B rings has a basis in the torsional angle energies. The MM3 energies depend extensively on the torsion angle components, θ, since they are modelled using a function of cos θ, cos 2θ, and cos 3θ. In a further decomposition, the torsion angles about C-2–O-5 were separated, as shown in Fig. 8. This indicates that the distinction between the flexibility of the two rings has its origin primarily in the large differences in the torsion angles about the C-2–O-5 bonds, which show a well-defined minimum at 72° (^3E) for the A-ring, while the B-ring has a broad minimum extending from 90° ($^3T_4$) to 254° (E_3), see Table 4.

Acknowledgements

We are grateful to Dr. J.R. Vercellotti of the Southern Regional Research Center for helpful discussions.

References

[1] R.U. Lemieux and R. Nagarajan, *Can. J. Chem.*, 42 (1964) 1270–1278.
[2] P.J. Anderson, *Biochim. Biophys. Acta*, 110 (1965) 627–629.

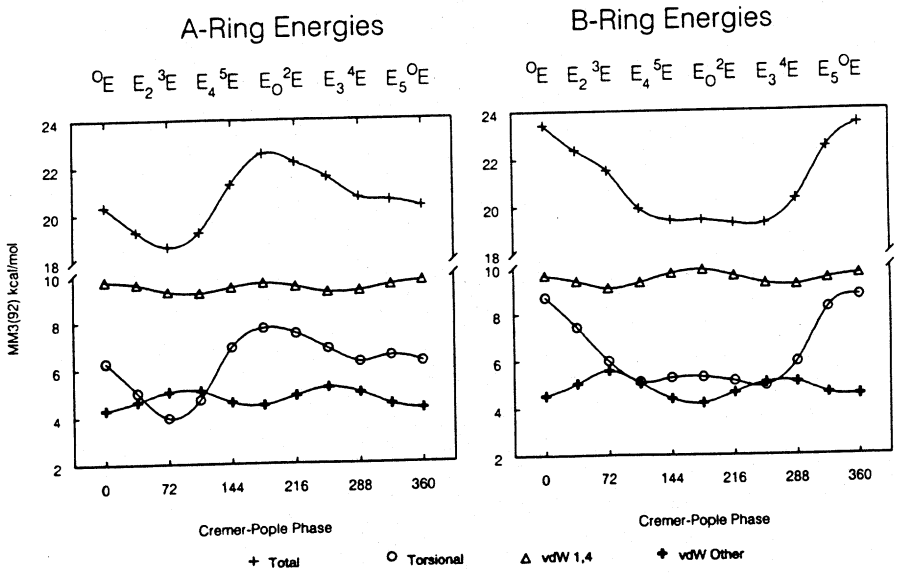

Fig. 8. Decomposition of the torsional energy components.

angular discrepancies between the model dihedral angles and the crystal values are 9° for both rings. For the NMR data the mean discrepancy is the same for the A ring, but larger, 14°, for the B ring. Since the NMR values correspond to a time average of the range of ring conformations, this is consistent with the greater flexibility of the B ring.

The results shown in Fig. 6 indicate that the principal difference between the A and B rings has a basis in the torsional angle energies. The MM3 energies depend extensively on the torsion angle components, θ, since they are modelled using a function of cos θ, cos 2θ, and cos 3θ. In a further decomposition, the torsion angles about C-2–O-5 were separated, as shown in Fig. 8. This indicates that the distinction between the flexibility of the two rings has its origin primarily in the large differences in the torsion angles about the C-2–O-5 bonds, which show a well-defined minimum at 72° (^3E) for the A-ring, while the B-ring has a broad minimum extending from 90° ($^3T_4$) to 254° (E_3), see Table 4.

Acknowledgements

We are grateful to Dr. J.R. Vercellotti of the Southern Regional Research Center for helpful discussions.

References

[1] R.U. Lemieux and R. Nagarajan, *Can. J. Chem.*, 42 (1964) 1270–1278.
[2] P.J. Anderson, *Biochim. Biophys. Acta*, 110 (1965) 627–629.

[3] J.B. Lambert, H.F. Shurvell, D.A. Lightner, and R.G. Cooks, *Introduction to Organic Spectroscopy*, Macmillan, New York, 1987.
[4] J.O. Lundgren, UPALS, A Full Matrix Least-Squares Refinement Program, Institute of Chemistry, University of Uppsala, Sweden, 1978.
[5] R.H. Blessing, BUFFALO, Medical Foundation of Buffalo, New York, USA, 1985.
[6] G.M. Sheldrick, SHELX86, Program for the Solution of Crystal Structures, University of Göttingen, Germany, 1986.
[7] MM3(92) is available from the Quantum Chemistry Exchange Program, Creative Arts Building, Indiana University, Bloomington, Indiana.